

## Effect of structural variation within cationic azo-surfactant upon photoresponsive function in aqueous solution

T. Hayashita<sup>1</sup>, T. Kurosawa<sup>2</sup>, T. Miyata<sup>2</sup>, K. Tanaka<sup>2</sup>, and M. Igawa<sup>2</sup>

<sup>1</sup> Department of Chemistry, Faculty of Science and Engineering, Saga University, 1 Honjo, Saga, Japan

<sup>2</sup> Department of Applied Chemistry, Faculty of Engineering, Kanagawa University, Kanagawa-ku, Kanagawa, Japan

**Abstract:** The cationic azo-surfactants possessing different spacers and tail alkyl chain lengths have been synthesized by azocoupling of *p*-alkylaniline or *o*-, *p*-ethoxyaniline with phenol, followed by alkylation and quaternalization with dibromoalkane and trimethylamine, respectively. These surfactants showed a good solubility in water. A reversible *trans-cis* isomerization of the azo-surfactants by photoirradiation was assessed by UV-Vis absorption spectra. Due to a difference in HLB between the *trans*- and *cis*-surfactants, the observed critical micelle concentration (CMC) values and the electric conductivity of the surfactant solution at above the CMC were significantly affected by the photoinduced *trans-cis* isomerization. The azo-surfactants bearing moderate alkyl chain lengths such as surfactants 6 ( $R_2 = C_2H_4$ ,  $R_3 = C_4H_9$ ) and 9 ( $R_2 = C_4H_8$ ,  $R_3 = C_2H_5$ ) were found to be effective to achieve large CMC changes (3.6 mmol/L for 6 and 5.9 mmol/L for 9) by UV-light irradiation. The replacement of the tail chain species also affected the photoresponsive function. The surfactant 12, possessing *p*-ethoxy group as the tail chain, was found to form a stable micelle aggregation as compared with the structurally related surfactant 10 having ethyl unit as its tail group, but it exhibited a large CMC change (5.3 mmol/L) by UV-light irradiation.

**Key words:** Cationic azo-surfactant – photoisomerization – electric conductivity – micelle formation – aggregation mode

### Introduction

Surfactant micelle solutions have been utilized in various analytical methods such as photometric analysis [1–4], extraction [5, 6], chromatography [7], ion-flotation [8–10], and so on. We believe, therefore, that the continuing development of surfactants possessing novel function must significantly contribute to an area of analytical chemistry. There are several factors affecting micelle formation in surfactant solution. In principle, a hydrophilicity-lipophilicity balance (HLB) of the surfactant governs the critical micelle concentration (CMC) as well as the aggregation mode of the micelle formation [11, 12]. The azobenzene compounds are known to exhibit *trans-cis* isomerization induced by photo-irradiation. A sym-

metrical *trans*-azobenzene is a nonpolar molecule while the bent *cis*-azobenzene is a polar molecule due to a large dipole moment across the azo-linkage [13–15]. When the azobenzene unit is introduced into the surfactant skeleton, a significant impact upon the HLB of the surfactant would be expected by photoisomerization, resulting in photocontrolled micelle formation.

A fundamental idea has already been reported by Shinkai et al. [16]. They prepared surfactants 1–3 containing an azobenzene unit (see Fig. 1) and showed that micelle formation was influenced by photoisomerization of the azo-surfactant on the basis of the above concept. However, their surfactants were not very soluble in aqueous solution which resulted in some unfavorable aggregation or precipitation during the experiments. Thus,

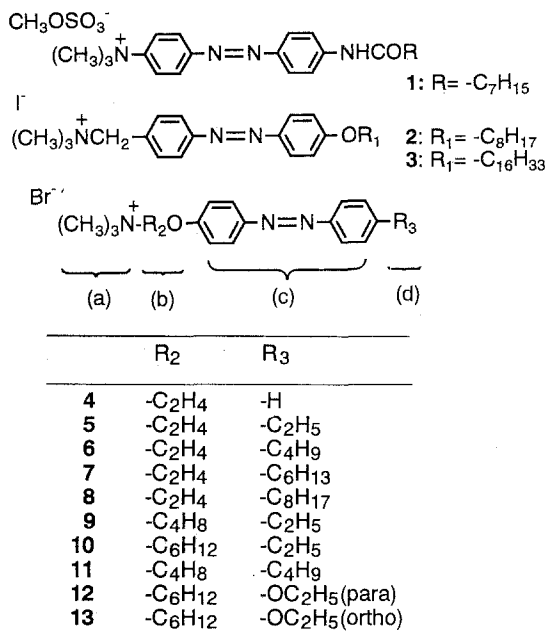


Fig. 1. Structure of azo-surfactants

they utilized a mixed micelle system with *N*-hexadecylpyridinium bromide in order to improve the solubility of the surfactants in aqueous solution. As a result, their system became quite complex and the influence of photoirradiation upon micelle formation was not as clear as would be expected from the *trans-cis* isomerization of the surfactants.

To understand a photoresponsive property of the azo-surfactant in aqueous solution, a precise design of the azo-surfactant is required. In this study, we synthesized new azo-surfactants 4–13 possessing photoresponsive function in aqueous media. As shown in Fig. 1, these surfactants have four main units: a) a trimethylammonium head group to provide a hydrophilic part of the surfactant, b) a spacer alkyl group ( $\text{R}_2$ ) to control a distance between the head group and the azobenzene unit, c) an azobenzene group as a photoresponsive site, and d) an alkyl tail group ( $\text{R}_3$ ) to provide the hydrophobic part of the surfactant. The positioning of the azobenzene unit in a surfactant can be altered by varying the combination of the spacer and the alkyl tail group length. By use of these azo-surfactants, the influences of structural variation within the azo-surfactants upon photoresponsive activation in aqueous micelle solution are examined and discussed.

## Experimental

### Apparatus

$^1\text{H}$ -NMR spectra were taken with a Hitachi R-24B (60 MHz) nuclear magnetic resonance spectrometer. UV-Vis spectra were measured with a Shimadzu UV-265 spectrophotometer. Elemental analysis data were obtained with a Perkin Elmer Model 240 CHN elemental analyzer. Conductivity measurements were performed with a Kyoto Electronics CM-117 conductivity meter and a K-121 conductivity cell including a thermistor for temperature calibration. Photoirradiation was carried out with an Ushio HB-50101 AA high-pressure mercury lamp.

### Reagents

Reagent-grade reactants and solvents were used as received from chemical suppliers. The azo-surfactants 4–13 were prepared by azocoupling of *p*-alkylaniline or *o*, *p*-ethoxyaniline with phenol, followed by alkylation and quaternalization with dibromoalkane and trimethylamine, respectively [17].

To ethanol–water solution (1:1, 50 mL) containing alkyylaniline (25.0 mmol) and sodium nitrite (25.0 mmol) in an ice bath, conc HCl (5 mL) and ice (25 g) were added. Then cold water containing phenol (25 mmol) and NaOH (50 mmol) was carefully added to the solution, and the mixture was stirred for 90 min. The pH of solution was adjusted to 1.0 with HCl and left to stand for 30 min. The resulting precipitate was filtered, washed with pure water, and dried under vacuum. The dried product (10 mmol) was dissolved in ethanol (50 mL) containing NaOH (25 mmol). To this solution, 20 mL of ethanol containing alkyldibromide (30 mmol) was added and refluxed for 8 h. The precipitated NaBr was removed by filtration and the filtrate was left to set for 1 day at room temperature. The precipitate was recovered, washed with cold ethanol, cold water, and then dried under vacuum. The dried product was dissolved in dry THF (100 mL) and trimethylamine gas was bubbled through the solution for 30 min, and the solution was left for 2 days. The resultant precipitate was filtered, washed with THF, and dried under vacuum. The product was recrystallized twice from ethanol.

*4-(Trimethylaminoethoxy) azobenzene bromide 4*: Yield 12% (orange powder).  $^1\text{H-NMR}$  ( $\text{D}_2\text{O}$ ):  $\delta_{\text{ppm}}$  3.3 (s, 9H), 3.5–4.1 (m, 4H), 7.8–8.0 (m, 9H). Anal. found: C, 56.45; H, 6.18; N, 11.55%. Calcd. for 4: C, 56.05; H, 6.09; N, 11.54%.

*4-Ethyl-4'-(trimethylaminoethoxy) azobenzene bromide 5*: Yield 19% (yellow powder).  $^1\text{H-NMR}$  ( $\text{CDCl}_3$ ):  $\delta_{\text{ppm}}$  1.2 (t, 3H), 2.3–2.9 (m, 2H), 3.6 (s, 9H), 4.1–4.7 (m, 4H), 6.8–8.0 (m, 8H). Anal. found: C, 57.41; H, 6.63; N, 10.59%. Calcd. for 5·1/4  $\text{H}_2\text{O}$ : C, 57.51; H, 6.73; N, 10.59%.

*4-Butyl-4'-(trimethylaminoethoxy) azobenzene bromide 6*: Yield 13% (yellow powder).  $^1\text{H-NMR}$  ( $\text{CDCl}_3$ ):  $\delta_{\text{ppm}}$  1.0 (t, 3H), 1.5–1.8 (m, 4H), 2.5–3.0 (m, 2H), 3.6 (s, 9H), 4.2–4.9 (m, 4H), 7.0–8.0 (m, 8H). Anal. found: C, 60.21; H, 7.42; N, 9.94%. Calcd. for 6: C, 60.00; H, 7.19; N, 10.00%.

*4-Hexyl-4'-(trimethylaminoethoxy) azobenzene bromide 7*: Yield 10% (yellow powder).  $^1\text{H-NMR}$  ( $\text{CDCl}_3$ ):  $\delta_{\text{ppm}}$  1.0–2.0 (m, 11H), 2.4–2.9 (m, 2H), 3.6 (s, 9H), 4.2–4.9 (m, 4H), 6.9–8.0 (m, 8H). Anal. found: C, 60.58; H, 7.84; N, 9.22%. Calcd. for 7·1/2  $\text{H}_2\text{O}$ : C, 60.39; H, 7.71; N, 9.19%.

*4-Octyl-4'-(trimethylaminoethoxy) azobenzene bromide 8*: Yield 14% (yellow powder).  $^1\text{H-NMR}$  ( $\text{CDCl}_3$ ):  $\delta_{\text{ppm}}$  0.7–1.9 (m, 15H), 2.4–3.0 (m, 2H), 3.7 (s, 9H), 4.3–5.0 (m, 4H), 7.0–8.3 (m, 8H). Anal. Found: C, 63.28; H, 8.06; N, 8.86%. Calcd. for 8: C, 63.02; H, 8.04; N, 8.82%.

*4-Ethyl-4'-(trimethylaminobutoxy) azobenzene bromide 9*: Yield 38% (yellow powder).  $^1\text{H-NMR}$  ( $\text{CDCl}_3$ ):  $\delta_{\text{ppm}}$  1.3 (t, 3H), 1.7–2.3 (m, 4H), 2.4–3.0 (m, 2H), 3.4 (s, 9H), 3.5–4.3 (m, 4H), 6.8–8.0 (m, 8H). Anal. found: C, 59.84; H, 7.38; N, 9.94%. Calcd. for 9: C, 60.00; H, 7.19; N, 10.00%.

*4-Ethyl-4'-(trimethylaminohexyloxy) azobenzene bromide 10*: Yield 30% (orange powder).  $^1\text{H-NMR}$  ( $\text{CDCl}_3$ ):  $\delta_{\text{ppm}}$  1.3 (t, 3H), 1.3–1.9 (m, 8H), 2.5–3.0 (m, 2H), 3.3–3.9 (m, 11H), 4.1 (t, 2H), 6.8–8.0 (m, 8H). Anal. found: C, 59.32; H, 7.63; N, 9.02%. Calcd. for 10· $\text{H}_2\text{O}$ : C, 59.22; H, 7.78; N, 9.01%.

*4-Butyl-4'-(trimethylaminobutoxy) azobenzene bromide 11*: Yield 13% (orange powder).  $^1\text{H-NMR}$  ( $\text{CDCl}_3$ ):  $\delta_{\text{ppm}}$  1.3 (t, 3H), 1.3–2.0 (m, 8H), 2.4–2.9 (m, 2H), 3.4 (s, 9H), 3.5–4.3 (m, 4H),

6.8–8.0 (m, 8H). Anal. found: C, 59.15; H, 7.79; N, 9.00%. Calcd. for 11· $\text{H}_2\text{O}$ : C, 59.22; H, 7.78; N, 9.01%.

*4-Ethoxy-4'-(trimethylaminohexyloxy) azobenzene bromide 12*: Yield 26% (yellow needle).  $^1\text{H-NMR}$  ( $\text{CDCl}_3$ ):  $\delta_{\text{ppm}}$  1.0–2.3 (m, 11H), 3.1–5.0 (m, 15H), 6.7–8.4 (m, 8H). Anal. found: C, 58.85; H, 7.36; N, 8.77%. Calcd. for 12·1/4  $\text{H}_2\text{O}$ : C, 58.91; H, 7.41; N, 8.96%.

*2-Ethoxy-4'-(trimethylaminohexyloxy) azobenzene bromide 13*: Yield 38% (brown powder).  $^1\text{H-NMR}$  ( $\text{CDCl}_3$ ):  $\delta_{\text{ppm}}$  1.3–2.2 (m, 11H), 3.3–3.7 (m, 11H), 3.8–4.5 (m, 4H), 6.7–8.0 (m, 8H). Anal. found: C, 60.04; H, 7.71; N, 9.10%. Calcd. for 13: C, 59.48; H, 7.38; N, 9.05%.

#### Measurements of photoisomerization

An aqueous solution (50 mL) of  $5.0 \times 10^{-5}$  mol/L of each surfactant was prepared. For UV-light irradiation, an aliquot (5 mL) of the solution was photoirradiated with a 500 W high pressure mercury lamp through a Toshiba UV-D35 glass filter ( $\lambda = 350 \pm 50$  nm) for 15 min. For Vis-light irradiation, the solution was photoirradiated with the same lamp through a Toshiba B46 glass filter ( $\lambda = 460 \pm 50$  nm) for 15 min. The UV-Vis spectra of the sample solutions were recorded 1) before photoirradiation (spectrum A), 2) after UV-light irradiation (spectrum B), and 3) after UV-light irradiation followed by Vis-light irradiation (spectrum C). A typical set of spectra A, B and C is shown in Fig. 2.

#### Measurements of critical micelle concentration (CMC)

An aqueous solution (50 mL) of  $2.0 \times 10^{-2}$  mol/L of each surfactant was prepared. Each sample solution was irradiated with UV-light until the electric conductivity of the solution exhibited a constant value. The sample solutions before and after the UV-light irradiation were diluted to an appropriate surfactant concentration and their conductivities were measured at 25 °C with a conductivity meter. The conductivities were plotted against the surfactant concentration and the CMCs were determined from a break point of the plots.

## Results and discussion

### Preparation of photoresponsive surfactants

The cationic surfactants containing an azobenzene unit were prepared by azocoupling of *p*-alkylaniline or *o,p*-ethoxyaniline with phenol, followed by alkylation and quaternalization with dibromoalkane and trimethylamine, respectively. The final products were purified by recrystallization from ethanol. The structure of the respective surfactants was identified by means of  $^1\text{H-NMR}$  measurements and elemental analysis (see the experimental section). Since the preparation conditions of the respective steps were not optimized, the overall yields of the surfactants were relatively low in our study.

### Photoisomerization of the surfactants

Azobenzene derivatives generally exist in the *trans*-form in solution. However, the energetically less-stable *cis*-conformer is formed by UV-light irradiation due to *trans-cis* isomerization [18]. This isomerization is monitored as a spectral change of the azo-surfactants. Figure 2 shows an example of UV-Vis spectra for surfactant 4. The *trans*-form of the azo-surfactant generally exhibits a maximum absorption band at ca. 350 nm in aqueous solution [16, 19]. In agreement, the

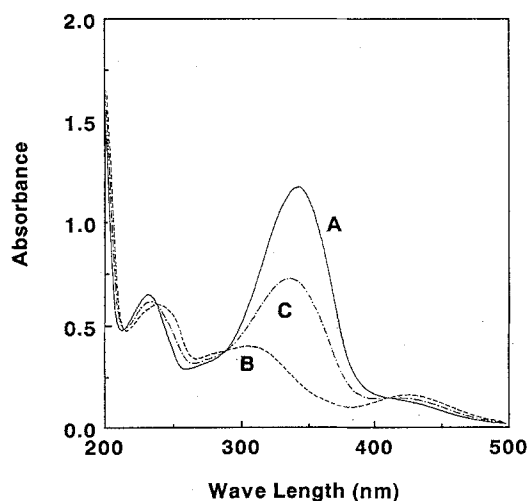


Fig. 2. Influence of photoirradiation upon absorption spectra of  $5 \times 10^{-5}$  mol/L 4 in aqueous solution. (A) Before UV-light irradiation, (B) after UV-light irradiation, and (C) after UV-light irradiation followed by Vis-light irradiation

absorption band recorded before UV-light irradiation showed a maximum at 344 nm (spectrum A). This band decreased after UV-light irradiation, and a weak absorption band based on  $n - \pi^*$  transition of *cis*-isomer appeared at about 440 nm (spectrum B). A photoequilibrium was established within 5 min and 84% *cis*-isomer was obtained after UV-light irradiation for 15 min. After UV-light irradiation, the sample was irradiated with Vis-light for 15 min and the UV-Vis spectrum was recorded in succession (spectrum C). After Vis-light irradiation, the absorption band at 344 nm due to the *trans*-isomer increased and three clear isosbestic points were observed at 242, 292, and 414 nm, respectively. This indicates that a reversible *trans-cis* isomerization was attained under the experimental condition. It should be noted, however, that the maximum absorption band at 344 nm did not fully recover even after a long (more than 30 min) Vis-light irradiation time. This indicates that the photo-stationary state of the *cis*-isomer remains to some extent in this system. A similar behavior was observed for all other surfactants. The molar extinction coefficient,  $\epsilon$ , for *trans*-isomers at maximum absorption band and the isosbestic points observed by photoirradiation are presented in Table 1. Most of  $\epsilon$  values ranged from 21 600 to 24 400  $\text{M}^{-1} \text{cm}^{-1}$ , in agreement with the reported values [16]. When the tail group was changed from ethyl to ethoxy groups, the  $\epsilon$  values decreased to 17 600 for 12 and 16 800 for 13, respectively.

Table 1. UV-Vis spectral characteristics of azo-surfactants 4–13

Surfactant	$\lambda_{\text{max}}$ (nm)	$\epsilon \times 10^3$ (L/mol cm)	IP (nm)		
			$\lambda_1$	$\lambda_2$	$\lambda_3$
4	344	23.0	242	292	414
5	348	24.2	245	303	420
6	350	22.4	246	303	424
7	349	23.3	246	305	425
8	347	24.4	244	300	425
9	352	23.5	246	304	427
10	352	23.4	245	306	428
11	353	21.6	247	306	430
12	359	17.6	255	320	441
13	358	16.8	252	312	— <sup>a</sup>

<sup>a</sup> Only two isosbestic points (IP) were observed.

### Electric conductivity change of surfactant solution

To elucidate a relationship of *trans-cis* isomerization with characteristics of these surfactants, we first investigated the influence of the UV-light irradiation upon the conductivity change of the surfactant solution. An aqueous solution (25 mL) containing  $2.0 \times 10^{-2}$  mol/L of each surfactant (sufficiently higher than CMC) was photoisomerized by UV-light irradiation and the electric conductivity of the solution was measured every 3 min. The resultant conductivity changes as a function of UV-light irradiation time are shown in Fig. 3. The conductivities due to presence of the *trans*-surfactants increased as the UV-light irradiation time was increased, and eventually reached a saturation value. The saturated value may be attributed to the conductivities of mixed micelles composed of both the *cis*- and *trans*-surfactant isomers. The initial conductivity ( $\kappa_i$ ) and the photoequilibrated conductivity ( $\kappa_{eq}$ ) are listed in Table 2 together with the UV-light irradiation time required for attainment of equilibrium. It is evident that the time required for the photoequilibrium increases as the alkyl chain length of the surfactant increases. This may be ascribed to a stable micelle formation by surfactants possessing longer alkyl chains, which disturbs a smooth *trans-cis* photoisomerization.

To understand the structural effect in the present surfactants, the conductivities observed for the respective micellar solutions were plotted against the alkyl chain length of the tail group and

Table 2. Electric conductivity change by UV-light irradiation

Surfactant	Conductivity ( $\mu\text{S}/\text{cm}$ )		Time <sup>a</sup> (min)
	$\kappa_i$	$\kappa_{eq}$	
4	1410	1580	24
5	1092	1597	27
6	548	1262	84
7	310	753	90
8	193	551	99
9	721	1525	66
10	549	1085	69
11	419	907	84
12	262	736	114
13	923	1364	72

<sup>a</sup> Time required for the photoequilibrium.

the spacer group (Fig. 4). When the spacer group length was fixed to ethylene and the tail group length was varied, i.e., as is seen for surfactants 4, 5, 6, 7 and 8, both the initial and the equilibrium conductivities decreased as the tail group length was increased (Fig. 4(a)). Figure 4(b) shows the influence of spacer chain length for surfactants with an ethyl tail group (surfactants 5, 9 and 10). A similar effect for the spacer length variation was noted. Thus, both  $\kappa_i$  and  $\kappa_{eq}$  decreased as the spacer group length was increased. The large differences between  $\kappa_i$  and  $\kappa_{eq}$  were observed for surfactant 6 ( $\Delta\kappa = 714 \mu\text{S}/\text{cm}$ ) and 9 ( $\Delta\kappa = 804 \mu\text{S}/\text{cm}$ ) which have moderate alkyl spacers

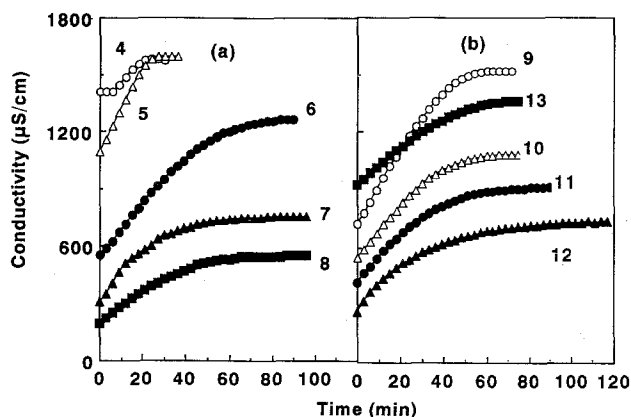


Fig. 3. Electric conductivity change of aqueous solution containing  $2.0 \times 10^{-2}$  mol/L surfactants a) 4–8 and b) 9–13 as a function of UV-light irradiation time at 25 °C

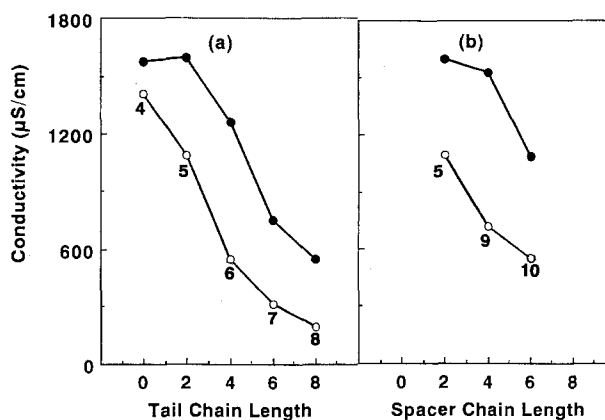


Fig. 4. Influence of a) tail and b) spacer group length upon electric conductivity. a) The spacer group was fixed to ethylene (Surfactants 4, 5, 6, 7 and 8). b) The tail group was fixed to ethyl (Surfactants 5, 9 and 10). (○) Before UV-light irradiation, (●) after UV-light irradiation. Surfactant concentration,  $2.0 \times 10^{-2}$  mol/L. Temperature, 25 °C

and tail chain lengths, respectively. The great difference in conductivity value at the same concentration ( $2 \times 10^{-2}$  mol/L) will be discussed later in terms of the difference in aggregation mode of surfactants.

#### Influence of UV-light irradiation on micelle formation

The increased conductivity observed upon UV-light irradiation may be due to a difference in the aggregation mode of the micelle formed from the *trans*-surfactant as compared to that of the *trans*, *cis*-surfactant mixture. To clarify the micelle formation behavior of each surfactant, the conductivity change of the surfactant solution was examined as a function of surfactant concentration. The conductivity, calibrated at 25 °C, was measured at each surfactant concentration by diluting a  $2 \times 10^{-2}$  mol/L surfactant solution of the *trans*-surfactant (without UV-light irradiation) and the *trans*-*cis* surfactant mixture (after photoequilibrium by UV-light irradiation).

Resultant conductivity changes for surfactants 4–8, and 9–13 are shown in Fig. 5, and 6, respectively. In all cases, the break points attributed to their CMC decreased as an alkyl chain length of the surfactant increased. A clear difference of the break point was commonly observed for all the azo-surfactant solutions of before and after UV-light irradiation. This behavior may be schemati-

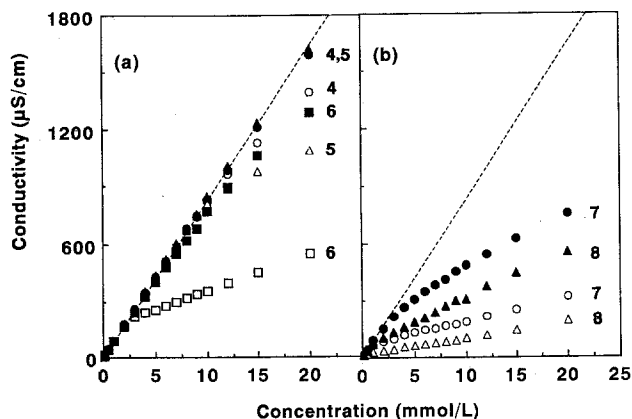


Fig. 5. Electric conductivity change as a function of surfactant concentration. a) (○, ●) 4, (△, ▲) 5, (□, ■) 6; b) (○, ●) 7, (△, ▲) 8. Open symbols, before UV-light irradiation; Closed symbols, after UV-light irradiation. Temperature, 25 °C

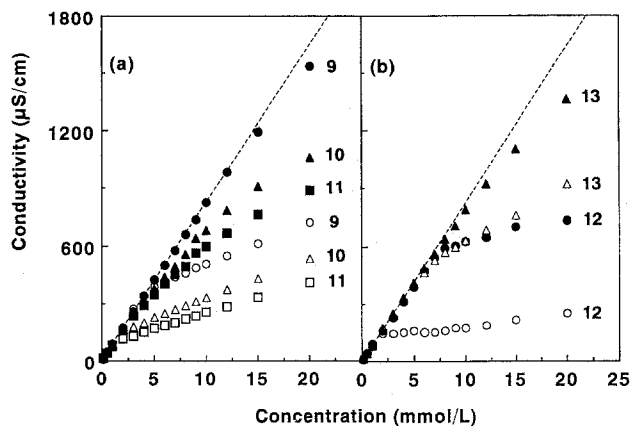


Fig. 6. Electric conductivity change as a function of surfactant concentration. a) (○, ●) 9, (△, ▲) 10, (□, ■) 11; b) (○, ●) 12, (△, ▲) 13. Open symbols, before UV-light irradiation; Closed symbols, after UV-light irradiation. Temperature, 25 °C

cally interpreted as shown in Fig. 7. In a dilute surfactant solution (A, A'), the surfactant molecules exist as a monomer molecular state and thus the conductivity of both *trans*- and *cis*-surfactant solution increases linearly with an increase of surfactant concentration. In such a concentration regions as B and B', micelle formation occurs for the *trans*-surfactant, while the *trans*, *cis*-surfactant mixture remains in their monomeric form due to the difference in their HLB. Thus the conductivity change of the *trans*-surfactant shows a lower break point and a slower slope of the curve appears due to its micelle formation compared with that of the solution after UV-light irradiation (*trans*-, *cis*-surfactant mixture). On the other hand, the conductivity of the *trans*, *cis*-surfactant mixture increases with the same slope as observed in region A and A'. Further increase of the surfactant concentration causes the subsequent micelle formation for *trans*, *cis*-surfactant mixture (C, C'). In this region, the conductivity change of the *trans*-*cis* surfactant mixture exhibits a break point corresponding to its CMC and a different slope appears with an increase of the surfactant concentration. The micelle solution after the UV-light irradiation showed a higher conductivity compared with the micelle solution of *trans*-surfactant, indicating that the aggregation pattern of the micelles is different between the *trans*-surfactant and the *trans*, *cis*-surfactant mixture, i.e., the mode of micelle formation is different between

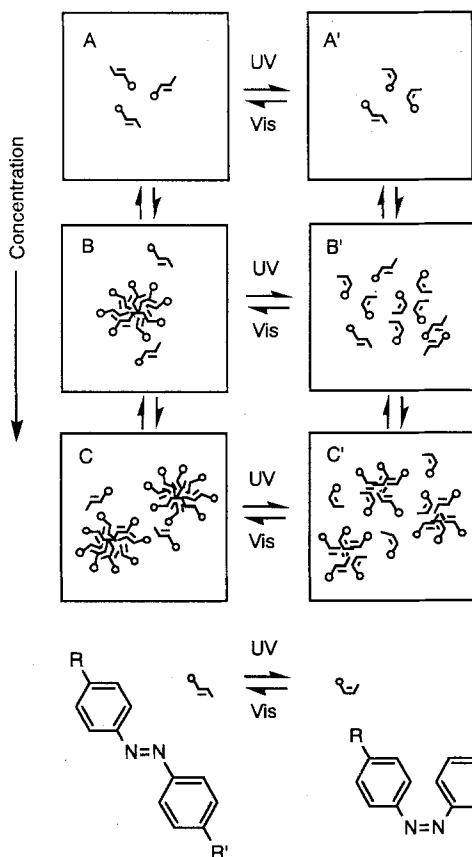


Fig. 7. Photoresponse mechanism of azo-surfactant solution

the *trans*-surfactant and the *trans*-, *cis*-surfactant mixture as for equilibrium (CMC), aggregation number, structure of micelles and so on. In more stable and/or larger micelles, the counter ions may be more tightly bound on the micelle surface; these must result in a lower conductivity of the solution. Thus, the photoresponsive conductivity change for azo-surfactant can be observed in the region of both B, B' and C, C'.

The observed CMC determined from the break points for 4–13 are listed in Table 3 together with  $\Delta\text{CMC}$  between before (dark) and after UV-light irradiation. In Figure 8 are shown the CMC change plotted against a) alkyl chain length of the tail group (the spacer group was fixed to ethylene, 4–8) and b) alkyl chain length of the spacer group (the tail group was fixed to ethyl, 5, 9, 10). In all cases, a higher CMC was noted for the surfactant solution after the UV-light irradiation. Figure 8(a) reveals that the CMC shifted to a lower concen-

Table 3. CMC change by UV-light irradiation

Surfactant	CMC (mmol/L)		
	dark	UV-light	$\Delta\text{CMC}$
4	10.5	11.5	1.0
5	9.5	11.5	2.0
6	2.4	6.0	3.6
7	0.7	2.1	1.4
8	0.3	0.8	0.5
9	4.6	10.5	5.9
10	1.6	3.0	1.4
11	1.2	2.7	1.5
12	1.7	7.0	5.3
13	6.3	9.4	3.1

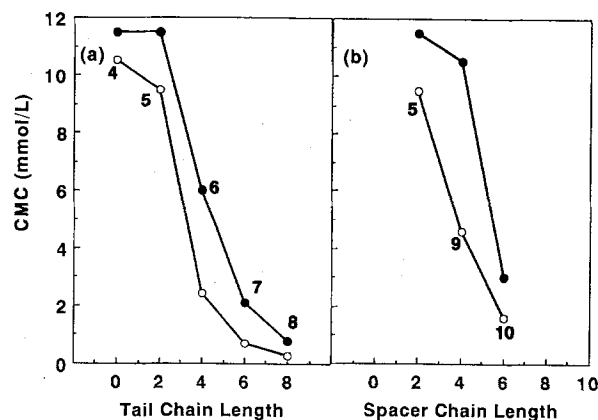


Fig. 8. Influence of a) tail and b) spacer group length upon CMC. a) The spacer group was fixed to ethylene. b) The tail group was fixed to ethyl. (○) Before UV-light irradiation, (●) after UV-light irradiation. Temperature, 25 °C

tration as the tail chain length was increased. The influence of spacer chain length upon the CMC is similar to that of the tail chain length. Thus, the CMC decreased as the alkyl chain of the spacer group was increased. Note that large CMC changes were obtained for surfactants 6 ( $\Delta\text{CMC} = 3.6 \text{ mmol/L}$ ) and 9 ( $\Delta\text{CMC} = 5.9 \text{ mmol/L}$ ) which have moderate alkyl spacers and tail chain lengths in their skeleton.

The surfactants 7, 10, and 11 are the structural isomers possessing the same molecular weight. The surfactant 7 has an ethyl group as the tail chain and a hexylene bridge as the spacer group, while surfactant 10 has a hexyl group as the tail

chain and an ethylene bridge as the spacer group. As an intermediate structure, the surfactant 11 has a butyl and a butylene bridge for both the tail and the spacer group, respectively. Thus, the effect of positioning of the azobenzene unit upon the CMC can be evaluated (Table 3). The CMC observed for 7 possessing a longer tail chain shifted to the lower concentration compared with that for 10 having a shorter tail chain, indicating that the alkyl chain length of the tail group has a stronger influence than does that of the spacer group with respect to its effect upon micelle formation. However, no significant difference in the  $\Delta$ CMC before and after the UV-light irradiation was noted for these structural isomers 7, 10, and 11. This may be attributed to the relatively low CMC values of these surfactants. In case of the structural isomers 6 and 9, the surfactant possessing a shorter tail chain (9) exhibited a higher CMC and a somewhat larger CMC difference after UV-light irradiation. This is in agreement with the conductivity changes observed in Fig. 4.

When the surfactants 12 and 13 which have *p*-ethoxy and *o*-ethoxy groups are examined as the structural isomer, some differences are noted in their micelle formation (Fig. 6(b)). Though the CMC for *trans*-12 was similar to that for *trans*-10 possessing an ethyl group as the tail chain, the slope observed after the CMC of *trans*-12 was much lower than that of *trans*-10 as well as all other *trans*-surfactants. This indicates that a stable micelle formation, resulting in a larger aggregation number and a stronger binding of the counter anions at the surface of micelle, takes place for *trans*-12. Even after the UV-light irradiation, the surfactant 12 showed a lower slope in comparison with other surfactant systems. This is presumably due to a structural nature of *p*-ethoxy group which stabilizes the micelle aggregation efficiently. A replacement of the ethoxy tail group from *p*-position to *o*-position caused a significant increase in CMC. The CMC observed for *trans*-13 (6.3 mmol/L) is comparable with that for 12 after UV-light irradiation (7.0 mmol/L). Similar to the *cis*-form of the surfactants, a bent structure of 13 apparently labilizes the micelle formation.

In the present experiments, the surfactant solutions ( $2.0 \times 10^{-2}$  mol/L) before and after the UV-light irradiation were diluted to each surfactant concentration, and their conductivities were examined. We already confirmed that a direct

UV- and Vis-light irradiation to the surfactant solutions above CMC (region B, B' and C, C' in Fig. 7) exhibited reversible conductivity changes similar to those observed in Figs. 5 and 6. It must be noted, however, that a degree of *trans-cis* photoisomerization in the micelle solution may be different from the monodispersed surfactant solution. The HPLC analysis is an effective method to evaluate these isomerization degrees in the different micelle solutions. The detail will be reported soon together with the thermodynamic data of these azo-surfactants.

## Conclusions

The cationic azo-surfactants possessing different spacers and tail chain lengths have been prepared and compared with their photoresponsive functions in aqueous solution. *Trans-cis* isomerization of the azo-surfactants by UV-light irradiation led to increase in the electric conductivity of the surfactant solution at above the CMC as well as their CMC values. This behavior were interpreted by the difference in aggregation mode of the micelle formation between the *trans*-surfactant and the *trans*-, *cis*-surfactant mixture. The study of structural variation within the azo-surfactants revealed that the surfactants 6 and 9 which have moderate alkyl spacers and tail chain lengths exhibited large CMC changes (3.6–5.9 mmol/L) by UV-light irradiation. The azo-surfactant 12 possessing *p*-ethoxy tail chain exhibited a large CMC change (5.3 mmol/L) by UV-light irradiation although it formed a stable micelle aggregation as compared with the structurally related other surfactants such as 10 and 13. These results demonstrate that a proper combination of the spacer and the tail chain length and a selection of the tail chain species (alkyl or alkoxy) are important factors affecting the photoresponsive function of the azo-surfactants in aqueous solution.

## Acknowledgements

The authors thank Professor K. Shirahama of Saga University for his helpful discussion. This research was partly supported by a Grant-in-Aid for Encouragement of Young Scientists from the Ministry of Education, Science and Culture of Japan.



## References

1. Falcon M, Cuiteras J, Izquierdo A, Prat MD (1993) *Talanta* 40:17
2. Soroka K, Vithanage RS, Phillips DA, Walker B, Dasgupta PK (1987) *Anal Chem* 59:629
3. Love LJC, Habarta JG, Dorsey JG (1984) *Anal Chem* 56:1132A
4. Watanabe H, Yamaguchi N (1984) *Bunseki Kagaku* 33:E211
5. Nakashio F, Goto M, Matsumoto M, Irie J, Kondo K (1988) *J Membr Sci* 38:249
6. Hayashita T, Bartsch RA, Kurosawa T, Igawa M (1991) *Anal Chem* 63:1023
7. Terabe S (1989) *Trends in Anal Chem* 8:129
8. Sebba F (1962) In: *Ion Flotation*. Elsevier, New York
9. Yamada K, Koide Y, Yamanokuchi H, Ohmura M, Shosenji H (1989) *Bull Chem Soc Jpn* 62:2867
10. Koide Y, Sakura K, Shosenji H, Yamada K (1990) *J Chem Soc Dalton Trans*:641
11. Shinoda K (1963) In: *Colloidal Surfactants*. Academic Press, New York
12. Tanford C (1979) In: *The Hydrophobic Effect*. John Wiley & Sons, Inc., New York
13. Birnbaum PP, Style DW (1954) *Trans Faraday Soc* 50:1192
14. Zimmermann G, Chow LY, Paik UJ (1958) *J Am Chem Soc* 80:3528
15. Beveridge DL, Jaffe HH (1966) *J Am Chem Soc* 88:1948
16. Shinkai S, Matsuo K, Harada A, Manabe O (1982) *J Chem Soc Perkin Trans II*:1261
17. Kunitake T, Okahata Y, Shimomura M, Yasunami S, Takarabe K (1981) *J Am Chem Soc* 103:5401
18. Yamamoto H, Nishida A (1985) *Nihon Kagakukaishi*: 2338
19. Kunitake T, Shimomura M, Iida K, Okahata Y, Kano K, Ogawa T (1983) *Nihon Kagakukaishi*:893

Received October 5, 1993;  
accepted April 7, 1994

## Authors' address:

Dr. Takashi Hayashita  
Department of Chemistry  
Faculty of Science and Engineering  
Saga University  
1 Honjo, Saga 840  
Japan